Astron. Astrophys. 322, 147–154 (1997)

ASTRONOMY
AND
ASTROPHYSICS

Age and mass of main sequence A-Type stars

R. Asiain, J. Torra, and F. Figueras

Departament d'Astronomia i Meteorologia, Universitat de Barcelona, Avda. Diagonal 647, E-08028, Barcelona, Spain

Received 16 July 1996 / Accepted 20 November 1996

Abstract. We study the individual assignation of stellar ages and masses of Main Sequence A type stars from Strömgren photometry and stellar evolutionary models. A detailed evaluation of the errors involved in the determination of these parameters is also presented; the range where typical errors are found is 10-30% in age, and 7-15% in mass.

A test using accurate data on fundamental parameters of detached, double lined eclipsing binary systems allows us to evaluate the efficiency of several sets of recent stellar evolutionary models in describing A type stars. The models that consider the overshooting effect on the convective layers have been found to be the most realistic.

Key words: stars: fundamental parameters – stars: HR diagram – stars: evolution – stars: early-type

1. Introduction

The kinematics of Main Sequence A type stars in the solar neighborhood shows certain particular features which cannot be explained by the classical theory of ellipsoidal velocity distribution. To analyze the mechanisms responsible for features such as the presence of moving groups, the strong vertex deviation, and the observed increase in velocity dispersion with age, large stellar samples are required with both accurate velocities and positions and precise physical data, especially ages and masses.

The imminent publication of the most accurate astrometric data ever measured –the Hipparcos mission observations– will constitute a clear advance in the first requirement; the new proper motions and trigonometric parallaxes together with the new radial velocities obtained from the ground will provide us with very accurate velocities and positions of stars in the solar neighborhood.

In most studies on the kinematic evolution of neighboring main sequence stars individual ages are not considered. Instead, mean ages assigned from spectral type are used (e.g. Jahreiss & Wielen, 1983; Gómez et al, 1990). Although this is a reasonable first approximation for very early type stars, the increase in age dispersion as more advanced spectral types are considered can strongly affect the conclusions derived. Here we study the individual assignation of ages and masses to Main Sequence and moderately evolved B, A and F type stars (Sect. 2) from their atmospheric parameters and a given set of stellar evolutionary models. Special care is taken with stars in the Overlap Region, where the correspondence between the pair (age, mass) and the atmospheric parameters is not univocal.

When dealing with large samples of stars both $uvby-\beta$ and Geneva photometric systems have proved to be efficient tools in the atmospheric parameter determination. Photometric indices, once dereddened, are taken as input parameters in $T_{\rm eff}$ and $\log\ g$ calibrations (e.g. Moon and Dworetsky, 1985, Napiwotzki et al., 1993, Kobi and North, 1990); a detailed description of the full procedure can be found in Figueras et al. (1991) and Jordi et al. (1994, 1996). On the other hand, Z can also be provided by $uvby-\beta$ and Geneva photometry, in which the δm_0 and Δm_2 indices, respectively, are very well correlated with [Fe/H] for spectral types A3 to G2 (Smalley, 1993; Berthet, 1990; North & Nicolet, 1990).

In Sect. 3 a detailed computation of the age and mass error assignation is developed, and the variation of these quantities as a function of the position of the star in the HR diagram is presented. Finally, in Sect. 4 fundamental values of radii and masses of detached, double-lined eclipsing binary systems allow us to select the most realistic stellar models from recent publications.

2. Determination of stellar age and mass

The evolution of a stellar model of initial mass M is normally presented as a collection of $\mathcal{N}$ fixed stages, regardless of the mass considered. We will refer to each of these stages of evolution as *Equivalent Evolutionary Phase*, or EEP (Praether 1976).

Let us suppose that the surface gravity ($\log\ g^*$), effective temperature ($T_{\rm eff}{}^*$) and metallicity (Z^*) of a star are available. The first step in the procedure to determine its age and mass consists in calculating a new set of stellar evolutionary models (SEM hereafter) at a metallicity $Z = Z^*$ through a linear interpolation between two sets of SEM at different metallicities. In Figure 1 the correctness of this procedure has been evaluated.

Send offprint requests to: R. Asiain

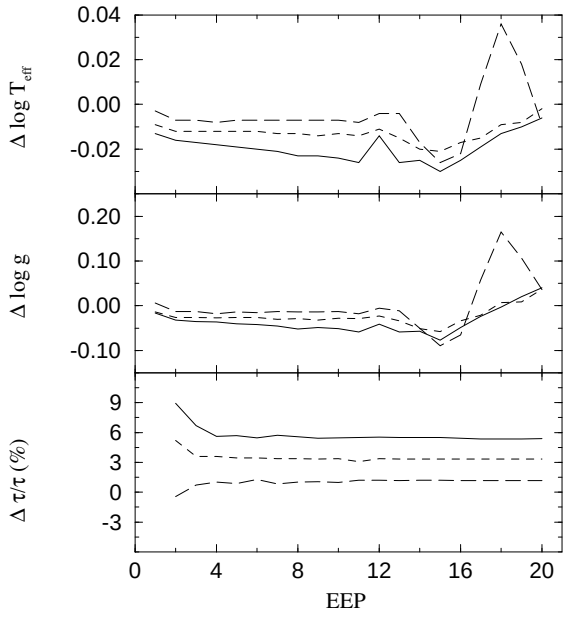

Fig. 1. Differences in $\log T_{\rm eff}$ (upper part), $\log\ g$ (middle part) and the relative differences in age (bottom part) between the theoretical stellar evolutionary models of SSMM (Table 1) at Z = 0.008 and the interpolated ones from models at Z=0.02 and Z=0.004. Calculations have been performed for the initial stellar masses M = 2 $M_{\odot}$ (*solid line*), 5 $M_{\odot}$ (*dashed line*) and 12 $M_{\odot}$ (*long dashed line*). The first EEP has been eliminated in the representation of $\Delta\tau/\tau$ since in this case the age is almost as small as the differences and, therefore, relative errors are too big

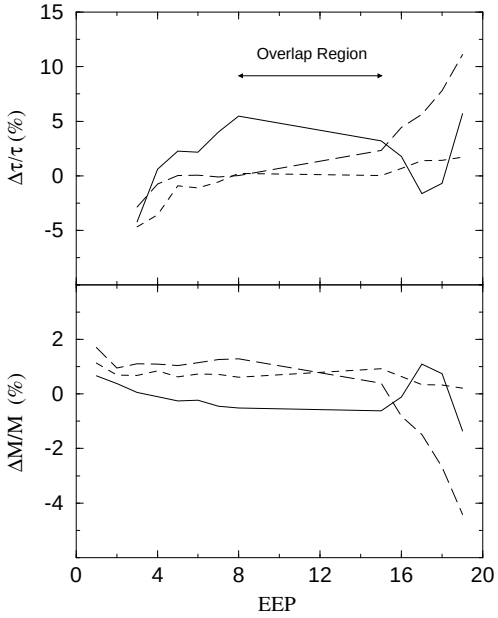

Fig. 2. Relative differences in age (upper part) and mass (bottom part) between original evolutionary tracks and interpolated ones. Calculations have been performed for the initial stellar masses $M_{\rm ZAMS}$ = 2 (*solid line*), 5 (*dashed line*) and 12 $M_{\odot}$ (*long dashed line*) using Schaller et al. (1992) models. The first EEP is not considered in the representation of $\Delta\tau/\tau$ for the same reason than in Figure 1

A set of interpolated models at Z=0.008 is in reasonably good agreement with the theoretical ones up to EEP point number 16 –transition towards the beginning of the helium burning phase– , while major differences appear near the Red Giant Branch for massive stars. So, the main uncertainty in this interpolation comes from the error in the observational determination of the stellar metallicity. When the test is repeated with a linear interpolation in $\log\ Z$ the differences are slightly larger than before, so we will adopt our first choice.

Once the set of evolutionary tracks at Z_* is computed, it is necessary to locate the HR diagram position of the star between two EEP and two evolutionary tracks. Details about the linear interpolation procedure –at a constant Z– to obtain stellar age, present mass and the mass at the moment of its birth ($M_{\rm ZAMS}$), are developed in Asiain (1993) and briefly described in the appendix A. As above, the procedure correctness is checked in Figure 2 –EEP points in the Overlap Region have been eliminated, since a special treatment has been devised for this region (see next subsection). The small differences in age ($<$5 %) and mass ($<$2 %) between theoretical and interpolated values prove the proper working of the procedure before the beginning of the Red Giant Branch.

The algorithm devised is applicable in all regions of the HR diagram where only one evolutionary phase is possible. For this reason, in the following subsection we study the specific assignation of ages and masses to stars in the Overlap Region, easily identifiable as a loop of the evolutionary tracks at the end of the Main Sequence. For stars at the Giant Branch or further evolutionary phases we face a problem that is analogous, though much more complicated, to that of the Overlap Region. Although the analytical method could provide a result, it would be highly unreliable because of the complexity of these regions. Stars that are close to the ZAMS have a big relative error in age, due to their small value of this parameter. The region below ZAMS is discussed in 2.2.

It is worthy to note that the determination of age is not very accurate for late type stars, for which a small uncertainty in $\log T_{\rm eff}$ or $\log\ g$ translates into a high error in age. On the other hand, since both atmospheric and stellar models commonly used pertain to *normal* stars, it is not possible to obtain accurate results either for fast rotating (very common among early type stars) or chemically peculiar stars, among others. Nevertheless, from an analysis of the Hyades cluster age we showed (Figueras et al., 1993) that the whole algorithm can be applied to metallic A type stars without introducing significant variations.

2.1. Overlap Region

At the very end of the Main Sequence, when hydrogen in the core of stars is almost consumed, the star initiates a contraction that produces an increase of its surface gravity and its effective temperature (Fig. 6). The contraction stops when a hydrogen burning shell appears around the star core. In this region of

the HR diagram there is no bijective relationship between [T_{eff}, log g] and [τ, M], and, as a consequence, a pair [T_{eff}, log g] can correspond to three different phases, namely:

A the Main Sequence phase. Stars spend much more time in this phase than in the other two;
B the contraction phase. Changes in the stellar structure are accelerated;
C the hydrogen burning shell phase. The evolution in this phase is even faster than in the previous case.

If we call τ_1, τ_2, τ_3 and M_1, M_2, M_3 the ages and masses of a star with atmospheric parameters T_{eff} and log g and evolutionary states A, B and C respectively, then:

$$\begin{aligned} \tau_1 &< \tau_2 < \tau_3 \\ M_1 &\geq M_2 \geq M_3 \end{aligned}$$

A solution to this problem consists in adopting the age and mass that corresponds to the most probable state (Grøsbol 1978). This state is defined taking into account the relative density of stars in each one of the three possible evolutionary phases. Since stars spend much more time in phase **A** than in **B** or **C**, they can be assumed to be in the Main Sequence, so for most of the stars in the Overlap Region (80–95 %) we would calculate the proper age and mass, while for the rest of them these values would deviated slightly but systematically from the real ones.

Instead, we prefer to weight the three possible results in order to obtain an unbiased mean age and mass for the whole sample. The weights for each of the three possible stages have been assumed to be proportional to the relative density of stars in them. The number of stars $\mathcal{N}_s$ born in (t, t+dt) with masses ranging from M to M+dM can be calculated from:

$$d\mathcal{N}_s = \phi(M)\, \psi(t)\, dM\, dt$$

where $\phi(M)$ is the Initial Mass Function (IMF), and $\psi(t)$ is the Star Formation Rate (SFR).

We suppose that the IMF profile is independent of t, at least during the short period that a star spends in one of the evolutionary states, and that its shape is given by:

$$\phi(M) = \phi_0\, M^{-(1+x)}$$

where the values of ϕ_0 and x depend on the mass M considered (we adopt the values given by Miller & Scalo 1979). We also assume that the SFR is constant from $t = \tau_1$ to $t = \tau_3$:

$$\psi(t) = C \quad (\tau_1 < t < \tau_3)$$

Then, the number of stars between two subsequent EEP points of the SEM of mass M_k can be described as:

$$\mathcal{N}_s^k = C\, \phi_0\, \Delta T\, M_k^{-(1+x)}$$

ΔT being the age difference between these two points. Introducing the number of stars per unit of length in the HR diagram, $\frac{\mathcal{N}_s^k}{d^k}$, where d^k is the distance in this diagram between the EEP points above defined, and a normalizing factor $\mathcal{Q}$, we can define the weights w_k as

$$w_k = \left[\frac{\mathcal{N}_s^k}{d^k}\right] \frac{1}{\mathcal{Q}} \quad \text{with } k = 1, 2, 3$$

The age and mass of any star located in the Overlap Region are derived from the following expressions:

$$\begin{aligned} \log \tau &= \sum_{k=1}^{3} w_k\, (\log \tau)_k \\ \log M &= \sum_{k=1}^{3} w_k\, (\log M)_k \end{aligned} \tag{1}$$

The ages and masses determined in this way are never equal to the values we would find if the evolutionary state of the star was known. However, since typical values of weights are much higher in the Main Sequence than in the other phases (appendix 5), the age assigned to a star in the Main Sequence state will not change appreciably, and only those stars in states **B** or **C** will have differences in age slightly higher than the observational errors.

2.2. Below the ZAMS

When photometry is used to obtain atmospheric parameters, the resulting T_{eff} and log g of a star sometimes place it below the ZAMS. This may be due either to errors on the photometric observations, to the existence of problems associated with the dereddening procedure or the computation of the atmospheric models, or to the presence of certain physical peculiarities (sometimes very difficult to detect). How can we determine the age or mass of a star that is outside the zone covered by the evolutionary tracks in the HR diagram? Actually, we cannot. However, we guess that all these stars are generally young ones, so we shift their position on the diagram –keeping their T_{eff} constant and varying their log g– until they cross the ZAMS. Then, their masses are interpolated between the first SEM points. Since in the first part of the evolution of a star its temperature does not change very much, there is a tight correlation between M and T_{eff}, so the M calculated in this way is presumably a good estimation. Nothing can be said about the age except that these stars may still be near the ZAMS.

3. Propagated errors

Errors related to the atmospheric parameters depend heavily on the procedure used to calculate them. Torra et al. (1990) compared the atmospheric parameters obtained from photometry with the fundamental ones in order to evaluate the errors, which can be considered external errors. For Main Sequence A type stars they found a mean error of 270 K in T_{eff}, and 0.18 dex in log g. In this section we take these last two values to study how these errors are propagated to the age and mass as a function of the position of the star in the HR diagram. The contribution

to the final error of the uncertainties in metallicity was not considered in the present work since δm_0-[Fe/H] relationship is defined only for stars later than A3 and the errors induced in the [Fe/H]-Z relationship remains somewhat uncertain (Strömgren, 1987).

In order to evaluate the effect of the uncertainties in effective temperature and surface gravities on the age and mass, we simulated a gaussian distribution of $\mathscr{M}$ points around the observed values (log T_{eff}, log g) of each star, adopting their corresponding individual errors as standard deviations. Applying our algorithm to these points we obtain a set of $\mathscr{M}$ ages and masses for each star; their dispersions are considered as the errors we finally assign to these variables. The dependence of these errors on the HR region where the star is placed is presented in Fig. 3. Errors in log τ have their maximum value near the ZAMS, where the age of stars is of the same order as its own error. The accuracy in the age determination drastically improves for stars slightly separated from the ZAMS. Except in the case of low temperatures, where the Main Sequence width is appreciably reduced, the most precise ages ($\approx$ 10% in age) are obtained around the position of the isochrone turnoff point; isochrones at these point are parallel to the log g-axis, so the large error in log g does not contribute significantly to the error in age. Another remarkable feature from Fig. 3 is that, as expected, the error in log τ increases when log T_{eff} decreases.

The fact that the real evolutionary phase of a star located in the Overlap Region is not known represents an additional uncertainty contributing to the final error for stars placed in this region. Thus, an estimation of this error ($\epsilon^{OR}_{\log\tau}$) has been computed as:

$$\epsilon^{OR}_{\log\tau} = \left(\epsilon(\log\tau)^2 + \sigma(\log\tau)^2\right)^{\frac{1}{2}} \quad (2)$$

where $\sigma(\log\tau)$ is the dispersion of the three possible star ages (τ_1, τ_2, τ_3) around the adopted value (see Sect. 2.1). The new error is easily seen in Fig. 3 as a discontinuity at the end of the Main Sequence.

The variation of the relative error in mass (Fig. 3) is much smaller than for log τ (less than $\sim$ 15%), basically due to the fact that errors in mass depend heavily on the slope of the evolutionary tracks in a log T_{eff}-log g diagram, and this slope does not change much in the Main Sequence and subsequent phases. As in the case of ages, ϵ_M/M in the Overlap Region has been calculated with an expression analogous to (2) in order to consider the phase uncertainty.

4. Comparing different stellar evolutionary models

During the last decades there have been several attempts to reproduce the evolution of stars, motivated, in part, by the increasing power of computers and the continuous improvement of the input physics. In Table 1 some of the most recent models are listed. Differences between them are due to the use of different physical ingredients in their calculation, such as the free parameter α of the mixing length theory for the convection treatment, the free parameter α_{over} which allows us to consider the effect

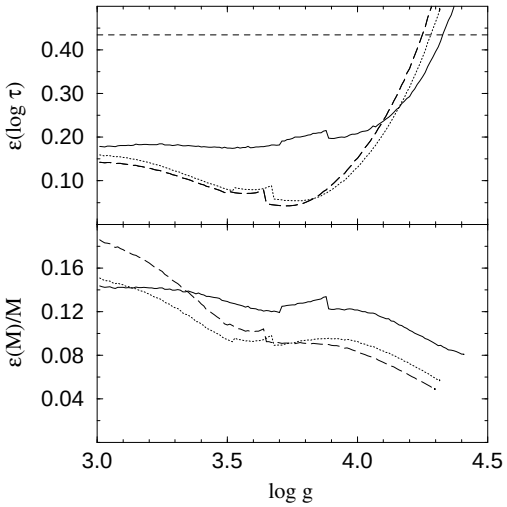

Fig. 3. Error in log τ and relative error in M along a line of constant effective temperature log T_{eff} = 3.8 (*solid line*), 4.0 (*dotted line*) and 4.2 dex (*long dashed line*). The horizontal *dashed line* in the upper graphic indicates an error in age of 100 % (SSMM models)

of overshooting as a mechanism to extend the convective shells, the nuclear reactions rates, the mean opacities, or the mass loss rates. Since the ages and masses obtained with our algorithm will depend on the SEM we use, a classical test has been developed to decide which of these recent models is more realistic. Comparison only consider solar composition models.

The most accurate information on fundamental parameters of stars (mass and radii) is obtained from the analysis of the light and radial-velocity curves of detached, double-lined eclipsing binary systems. Based on Andersen's (1991) and Popper's (1980) compilations of these kinds of binary stars, we constructed a sample of 61 stars with masses between 1 and 3 $M_\odot$, covering in this way the Main Sequence A-type range. According to Andersen (1991) the mean precision in *R* and *M* is 1.5 % and 1.4 % respectively. The log T_{eff} for these stars, coming from spectroscopic and photometric measurements from several authors, is more poorly determined (0.013 dex).

From R and M a very accurate log g can be computed (mean error of 0.015 dex). Similarly to the appendix, log M allows to linearly interpolate an evolutionary track among a set of SEM, whereas log g is used to interpolate the log age (log τ) and effective temperature (log$T_{eff}{}^c$) between two EEP inside this evolutionary track for every component of each binary system. These two new values are very precise too; they will constitute the key to our SEM test.

The main evaluation of the models of Table 1 is based on the hypothesis of "same age" for the two components of every binary system. We define $\Delta\log\tau$ as follows:

$$\Delta\log\tau = \frac{\sum_{i=1}^{\mathscr{P}} \omega_i \mid \log\tau_{1,i} - \log\tau_{2,i} \mid}{\sum_{i=1}^{\mathscr{P}} \omega_i}$$

Table 1. Main characteristics of some of the most recent stellar evolutionary models. LAOL= Los Alamos Opacity Library (Huebner et al. 1977); OPAL= Opacity Library by Rogers & Iglesias (1992). †*The core overshooting parameter is* $\alpha_{\rm over,c}$ *= 0.25 in the mass range 1.0* $\leq M \leq$ *1.5, and* $\alpha_{\rm over,c}$ *= 0.50 above it; the envelope overshoot is* $\alpha_{\rm over,e}$ *= 0.7 all over the mass range*

Models	(Y, Z)	α	$\alpha_{\rm over}$	Mass range	Opacities	Reference
VAN	0.250 0.0170	1.60	0.00	0.70 - 3	LAOL	VandenBerg (1985)
MM	0.280 0.0200	1.90	0.25	0.85 - 120	LAOL	Maeder & Meynet (1989)
CCS	0.270 0.0200	1.60	0.00	0.60 - 9	LAOL	Castellani et al. (1992)
CG	0.267 0.0100	1.50	0.20	1.00 - 40	OPAL	Claret & Giménez (1992)
	0.280 0.0200	1.50	0.20	1.00 - 40	OPAL	Claret & Giménez (1992)
	0.321 0.0300	1.50	0.20	1.00 - 40	OPAL	Claret & Giménez (1992)
SSMM	0.243 0.0010	1.60	0.20	0.80 - 120	OPAL	Schaller et al. (1992)
	0.252 0.0040	1.60	0.20	0.80 - 120	OPAL	Charbonnel et al. (1993)
	0.264 0.0080	1.60	0.20	0.80 - 120	OPAL	Schaerer et al. (1993a)
	0.300 0.0200	1.60	0.20	0.80 - 120	OPAL	Schaller et al. (1992)
	0.360 0.0400	1.60	0.20	0.80 - 120	OPAL	Schaerer et al. (1993b)
BFBC	0.230 0.0004	1.63	0.25†	0.60 - 120	OPAL	Fagotto et al. (1994a)
	0.240 0.0040	1.63	0.25†	0.60 - 120	OPAL	Fagotto et al. (1994b)
	0.250 0.0080	1.63	0.25†	0.60 - 120	OPAL	Fagotto et al. (1994b)
	0.280 0.0200	1.63	0.25†	0.60 - 120	OPAL	Bressan et al. (1993)
	0.352 0.0500	1.63	0.25†	0.60 - 120	OPAL	Fagotto et al. (1994a)

where $\mathscr{P}$ is the number of binary systems in our sample, ω_i are weights given by

$$\omega_i = [\epsilon^2(\log \tau_{1,i}) + \epsilon^2(\log \tau_{2,i})]^{-1}$$

and $\epsilon(\log \tau_{1,i})$ and $\epsilon(\log \tau_{2,i})$ are the errors propagated directly from the individual errors in R and M, as in Sect. 3. These weights prevent the very uncertain ages –such as those of stars near the ZAMS– from biasing the result.

In addition, the comparison between $\log T_{\rm eff}{}^c$ and the observed value $\log T_{\rm eff}$ gives us a secondary test. Let us define $\Delta \log T_{\rm eff}$ as:

$$\Delta \log T_{\rm eff} = \frac{\sum_{j=1}^{\mathscr{N}} \mid \log T_{{\rm eff},j} - \log T^{c}_{{\rm eff},j} \mid}{\mathscr{N}}$$

where $\mathscr{N}$ is the number of stars. The use of weights in this case is not recommended, since in practice they depend on the errors in the determination of the observational $T_{\rm eff}$, which are quite arbitrarily estimated.

The smaller $\Delta \log \tau$ and $\Delta \log T_{\rm eff}$ are, the closer the agreement between the SEM and these accurate observations. In fact, the first quantity is more reliable since it has been calculated solely from fundamental stellar parameters.

After rejecting ten stars located below the ZAMS we calculated $\Delta \log \tau$ and $\Delta \log T_{\rm eff}$ for three subsamples to evaluate the SEM fit in different HR-diagram regions:

i The whole sample (51 stars): it will show us the general fit in the 1 to 3 $M_\odot$ range;

ii Stars more massive than 1.5 $M_\odot$ (42 stars), excluding in this way the stars located in the conflictive Main Sequence transition between radiative and convective cores;

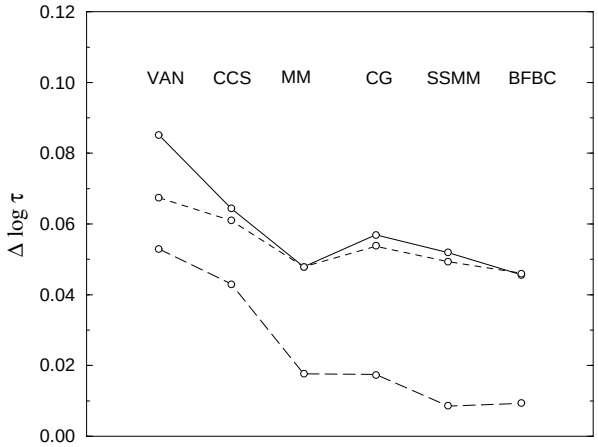

Fig. 4. $\Delta \log \tau$ as a function of different SEM. *Solid line*: the whole sample of eclipsing binary systems; *dashed line*: stars more massive than 1.5 $M_\odot$; *long-dashed line*: moderately evolved binary systems (see text)

iii Six moderately evolved binary systems, already analyzed by Andersen et al. (1990). This subsample will allow us to evaluate the importance of the overshooting effect, since the stars in it may be classified as Main Sequence or Subgiant branch stars as a function of the adopted $\alpha_{\rm over}$ value.

Fig. 4 shows the $\Delta \log \tau$ for different SEM. It is obvious from this figure that those models that do not take into account the overshooting effect on the convective layers (VAN and CCS) assign quite different ages to the components of the binary systems, especially for the most evolved ones [sample **iii**]. This is related to the fact that the overshooting effect tends to widen the

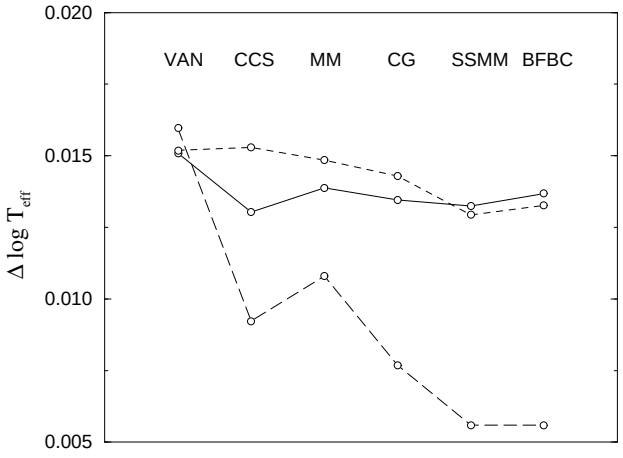

Fig. 5. Δ log$T_{\rm eff}$ for different SEM. Line style like in Fig. 4

HR-diagram. Results obtained with samples **i** and **ii** are almost equal, which indicates that the fit of the observations does not depend on the mass range. These results suggest that the behavior of all models with $\alpha_{\rm over} \neq 0$ (MM, SSMM, CG and BFBC) in this range of masses is, for the regions tested, very similar.

The general $T_{\rm eff}$ fit does not change markedly for samples **i** and **ii** when different SEM are considered, so it is independent of the mass (Fig. 5). For evolved stars (sample **iii**) the fit is clearly improved when the overshooting effect is included. The better fit obtained for moderately evolved stars (sample **iii**) is a consequence of their position in the HR diagram, far from the regions where errors are large.

From left to right, the general trend in Figs. 4 and 5 is to improve the match between observational information and the set of SEM, which almost implies a chronological improvement. An important contribution to this improvement is the application of the overshooting effect to better define the limits of the convective regions of stars. In particular, the best fits are obtained for SSMM and BFBC models. Some new studies on dynamo action in stratified convection with overshooting (Nordlund et al., 1992) and rotational effect on convection (Pulkkinen et al., 1993) will introduce important advances in the description of stellar evolution in the near future.

5. Conclusions

We have presented a procedure that allows us to determine the age and mass, and their corresponding errors, in a HR region where only one evolutionary phase is possible (e.g., Main Sequence), considering that their metallicity, effective temperature and surface gravity are known. As a first step, the algorithm interpolates, by means of the stellar metallicity, a set of stellar evolutionary models among other sets of published models at different metallicities, which allows us to work at the appropriate chemical composition. A second interpolation procedure is followed to determine age and mass from the new set of models. A complementary analysis is performed to extend the method to stars in the Overlap Region, where more than one evolutionary phase is compatible with a given temperature and gravity. A MonteCarlo simulation has been applied to evaluate the errors propagated from atmospheric parameters (errors in metallicity are not considered, though they should not significantly affect the results obtained for A type stars). Typical errors in ages are between 10 and 30% –increasing considerably when approaching the ZAMS– and between 7 and 15% in mass.

Some of the most recent sets of stellar evolutionary models are compared with the aid of very accurate data from detached, double lined eclipsing binary systems. Models that consider the overshooting effect on the limits of the convective layers are more compatible with the precise data than the others. In particular, our tests indicate that BFBC and SSMM models are the most realistic. Further work is currently been done to introduce metallicity as a new variable in our test to evolutionary models (Ribas et al., 1997).

The procedure presented here can probably provide sufficiently good ages and masses for Main Sequence B and F type stars, although high rotational velocities –for B stars– and uncertainties in the metallicity determination –for F stars– may considerably affect the results.

Acknowledgements. We thank Dr. Álvaro Giménez, Dr. Antonio Claret, Dr. Georges Meynet and Dr. Daniel Schaerer for their useful suggestions. This work has been supported by CICYT under contract PB95-0185 and by the Acciones Integradas Hispano-Francesas (HF95/328B). R.A. acknowledges financial support from the Ministerio de Educación y Ciencia.

Appendix A: interpolation of ages and masses among SEM

Suppose that the effective temperature (x^*), surface gravity (y^*) and metallicity (Z^*) of a star are known parameters. As described in Sect. 2, we can then determine a new set of SEM at Z^*. Let $x_{i,j}$, $y_{i,j}$, $\tau_{i,j}$ and $M_{i,j}$ be the log $T_{\rm eff}$, log g, age and mass, respectively, of the jth EEP of a track with initial mass $M_{i,1}$ when using this new set of SEM, and suppose that our star is contained in the HR region limited by tracks i and $i+1$, and EEPs j and $j+1$ (Fig. 6).

As a first approximation, it can be assumed that log $T_{\rm eff}$, log g, log τ and log M vary linearly with log $M_{i,1}$ inside a given EEP (j). Then, we can construct a new track with initial mass M_1^*,

$$x_j^{\rm int} = x_{i+1,j} + f_m\,(x_{i,j} - x_{i+1,j}) \quad \text{(A1)}$$

$$y_j^{\rm int} = y_{i+1,j} + f_m\,(y_{i,j} - y_{i+1,j}) \quad \text{(A2)}$$

$$\log \tau_j^{\rm int} = \log \tau_{i+1,j} + f_m\,(\log \tau_{i,j} - \log \tau_{i+1,j}) \quad \text{(A3)}$$

$$\log M_j^{\rm int} = \log M_{i+1,j} + f_m\,(\log M_{i,j} - \log M_{i+1,j}) \quad \text{(A4)}$$

where

$$f_m = \frac{\log M_1^* - \log M_{1,i+1}}{\log M_{1,i} - \log M_{1,i+1}} \quad \text{(A5)}$$

We also assume that log $T_{\rm eff}$, log g, and log M vary linearly with the age between two EEP points inside a given track. The

Table 2. For different pairs (log T_{eff}, log g) covering the Overlap Region in the A-type range the difference between the assigned values for $\log\tau$ ($\delta\log\tau$) and M (δM) –first and second columns respect.– and the corresponding values calculated as if the phase (**A**, **B** or **C**) where the star is was known. In the third column the probabilities of being to each phase are given

log g		log T_{eff}											
		4.2			4.1			4.0			3.9		
		$\delta\log\tau$	δM	w_k									
3.35	**A**	0.003	-0.017	90.5									
	B	-0.027	0.160	9.2									
	C	-0.049	0.315	0.3									
3.40		0.008	-0.042	87.1									
		-0.051	0.279	12.6									
		-0.058	0.314	0.3									
3.45		0.012	-0.064	85.9	0.005	-0.016	88.5						
		-0.076	0.395	13.1	-0.035	0.119	11.0						
		-0.067	0.329	1.0	-0.060	0.226	0.5						
3.50		0.006	-0.029	95.5	0.009	-0.030	87.9	0.013	-0.030	44.8			
		-0.122	0.613	3.3	-0.065	0.217	11.6	-0.010	0.023	54.9			
		-0.121	0.607	1.2	-0.067	0.222	0.5	-0.059	0.165	0.3			
3.55					0.013	-0.041	88.2	0.009	-0.021	87.7	0.005	-0.009	88.3
					-0.097	0.311	10.6	-0.065	0.146	11.5	-0.036	0.056	10.6
					-0.088	0.267	1.2	-0.077	0.177	0.8	-0.090	0.162	1.1
3.60								0.006	-0.013	95.1	0.012	-0.018	87.0
								-0.115	0.249	3.4	-0.080	0.118	11.9
								-0.109	0.230	1.5	-0.100	0.155	1.1
3.65											0.007	-0.010	95.0
											-0.143	0.205	3.9
											-0.122	0.165	1.1

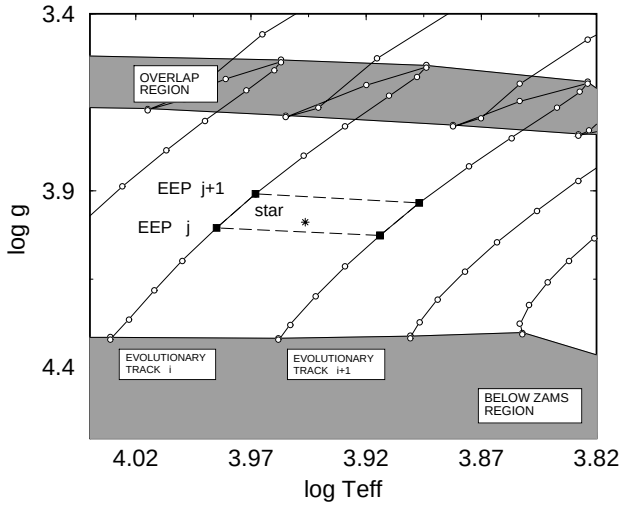

Fig. 6. Model points considered in the interpolation of the age and mass

log T_{eff} and log g of our star can then be calculated as

$$x^* = x_j^{\rm int} + f_\tau\,(x_{j+1}^{\rm int} - x_j^{\rm int}) \quad \text{(A6)}$$

$$y^* = y_j^{\rm int} + f_\tau\,(y_{j+1}^{\rm int} - y_j^{\rm int}) \quad \text{(A7)}$$

$$\log M^* = \log M_j^{\rm int} + f_\tau\,(\log M_{j+1}^{\rm int} - \log M_j^{\rm int}) \quad \text{(A8)}$$

f_τ being the interpolation factor along an evolutionary track

$$f_\tau = \frac{\tau - \tau_j^{\rm int}}{\tau_{j+1}^{\rm int} - \tau_j^{\rm int}} \quad \text{(A9)}$$

Equations (A6) and (A1) allow us to express the interpolation factor f_m as

$$f_m = \frac{x^* - x_{i+1,j} - f_\tau\,(x_{i+1,j+1} - x_{i+1,j})}{x_{i,j} - x_{i+1,j} + f_\tau\,(x_{i,j+1} - x_{i+1,j+1} - (x_{i,j} - x_{i+1,j}))} \quad \text{(A10)}$$

Introducing (A2) and (A10) in (A7), we obtain a second degree equation in f_τ

$$a f_\tau^2 + b f_\tau + c = 0$$

whose coefficients are given by

$$a = \Delta x_1 \Delta y_2 - \Delta y_1 \Delta x_2$$
$$b = \Delta x_1 \Delta y_{12} - \Delta y_1 \Delta x_{12} + \\ + \Delta y^* (\Delta x_2 - \Delta x_1) - \Delta x^* (\Delta y_2 - \Delta y_1)$$
$$c = \Delta y^* \Delta x_{12} - \Delta x^* \Delta y_{12}$$

and

$$\Delta x_1 = x_{i,j+1} - x_{i,j}$$
$$\Delta x_2 = x_{i+1,j+1} - x_{i+1,j}$$

$$\Delta y_1 = y_{i,j+1} - y_{i,j}$$
$$\Delta y_2 = y_{i+1,j+1} - y_{i+1,j}$$
$$\Delta x_{12} = x_{i+1,j} - x_{i,j}$$
$$\Delta y_{12} = y_{i+1,j} - y_{i,j}$$
$$\Delta x^* = x^* - x_{i+1,j}$$
$$\Delta y^* = y^* - y_{i+1,j}$$

Since a, b and c can be calculated using SEM and the T_{eff} and log g of the star, we can easily determine the roots of the quadratic equation, and from them, by means of Eq. (A10), we also determine the f_m values. We can then choose the proper solutions by just imposing the conditions

$$0 < f_m < 1$$
$$0 < f_\tau < 1$$

Once f_m is known, Eq. (A5) allows us to determine the initial mass of our star and, from Eqs. (A4) and (A8), its current mass. Finally, the age is determined by means of Eqs. (A3), (A5) and (A9).

Appendix B: ages, masses and weighting factors in the Overlap Region

Mean ages and masses have been calculated for stars placed in the Overlap Region following expressions 1. Typical differences between computed values and those we would assign if evolutionary phases were known are shown in Table 2 as a function of the position in the HR diagram.

References

Andersen J., 1991, A&AR 3, 91
Andersen J., Clausen J.V., Nordström B., 1990, ApJ 363, L33
Asiain R., 1993, Degree in Physics, Barcelona Univ.
Berthet S., 1990, A&A 236, 440
Bressan A., Fagotto F., Bertelli G., Chiosi C., 1993, A&AS 100, 647
Castellani V., Chieffi A., Straniero O., 1992, ApJS 78, 517
Charbonnel C., Meynet G., Maeder A., Schaller G., Schaerer D., 1993, A&A 101, 415
Claret A., Giménez A., 1992, A&AS 96, 255
Fagotto F., Bressan A., Bertelli G., Chiosi C., 1994a, A&AS 104, 365
Fagotto F., Bressan A., Bertelli G., Chiosi C., 1994b, A&AS 105, 29
Figueras F., Torra J., Jordi C., 1991, A&AS 87, 319
Figueras F., Torra J., Jordi C., Asiain R., 1993. In: Dworetsky M.M., Castelli F., Faraggiana R. (eds.), Peculiar Versus Normal Phenomena in A-type and Related Stars, PASPC 44, p. 634
Gómez A.E., Delhaye J., Grenier S., Jaschek C., Arenou F., Jaschek M., 1990, A&A 236, 95
Grøsbol P.J., 1978, A&AS 32, 409
Huebner W.F., Merts A.L., Magee N.H. Jr., Argo M.F., Eds. 1977, Astropys. Opacity Library, UC-346
Jahreiss H., Wielen R., 1983, Kinematics and Ages of Nearby Stars. In: A.G.D. Philip and A.R. Upgren (eds.), The Nearby Stars and the Stellar Luminosity Function, L. Davis Press. Schenectady, New York, p. 277
Jordi C., Masana E., Figueras F., Torra J., Asiain R., 1994, Space Science Reviews 66, 203
Jordi C., Figueras F., Torra J., Asiain R., 1996, A&AS 115, 401
Kobi D., North P., 1990, A&AS 85, 999
Maeder A., Meynet G., 1989, A&A 210, 155
Miller G.E., Scalo J.M., 1979, ApJ 41, 513
Moon T.T., Dworetsky M.M., 1985, MNRAS 217, 305
Napiwotzki R., Schönberner D., Wenske V., 1993, A&A 268, 653
North P., Nicolet B., 1990, A&A 228, 78
Nordlund A., Brandenburg A., Jennings R.L., Rieutord M., Ruokolainen J., Stein R. F., Tuominen I., 1993, A& A 267, 265
Popper D.M., 1980, ARA&A 18, 115
Prather M.J., 1976, PhD thesis, Yale Univ.
Pulkkinen P., Tuominen I., Brandenburg A., Nordlund A., Stein R.F., 1993, A&A 267, 265
Ribas I., Jordi C., 1997, A&A in preparation
Rogers F.J., Iglesias C.A., 1992, ApJS 79, 507
Schaller G., Schaerer D., Meynet G., Maeder A., 1992, A&AS 96, 269
Schaerer D., Meynet G., Maeder A., Schaller G., 1993a, A&AS 98, 523
Schaerer D., Charbonnel C., Meynet G., Maeder A., Schaller G., 1993b, A&AS 102, 339
Strömgren B., 1987. In: G. Gilmore and B.Carswell (eds.), The Galaxy, NATO ASI Series 207, p. 229
Smalley B., 1993, A&A 274, 391
Torra J., Figueras F., Jordi C., Rosselló G., 1990, Ap&SS 170, 251
VandenBerg D.A., 1985, ApJS 58, 771

This article was processed by the author using Springer-Verlag LaTeX A&A style file *L-AA* version 3.